JOURNAL OF GUIDANCE, CONTROL, AND DYNAMICS
Vol. 31, No. 4, July–August 2008

Engineering Notes

ENGINEERING NOTES are short manuscripts describing new developments or important results of a preliminary nature. These Notes should not exceed 2500 words (where a figure or table counts as 200 words). Following informal review by the Editors, they may be published within a few months of the date of receipt. Style requirements are the same as for regular contributions (see inside back cover).

Fuel-Efficient Formation Flight-Control Design Based on Energy Maneuverability

Jongug Choi* and Youdan Kim†
Seoul National University, Seoul 151-742, Republic of Korea

DOI: 10.2514/1.34351

I. Introduction

WHEN aircraft fly in formation, each aircraft takes advantage of the upwash of air coming off of the aircraft in front of it to reduce its workload. By flying in the area of the upwash, a follower aircraft can gain aerodynamic efficiency, which leads to fuel saving [1–3]. To achieve the fuel saving, the follower aircraft must fly in tight formation in which lateral separation between the leader and follower aircraft is less than a wingspan of the leader aircraft [4]. Because of the fuel saving effect, several research efforts have been focused on tight formation flying. In Chichka et al. [5], the peak-seeking control scheme was used to optimize the drag benefit during the flight. Pachter et al. [4] treated the tight formation maintenance problem for the maneuvering aircraft using linear kinematics. Additionally, a nonlinear controller was designed, taking into account nonlinearities that are typical of formation control dynamics [6].

Considering the operational requirements to enhance the mutual survivability in a threat environment, the tight formation geometry may not be suitable. For example, in the case of combat aircraft performing air patrol missions in the threat area, the formation geometry is decided based on the surface-to-air and air-to-air threats of the enemy. This tactical formation geometry is a loose formation in which the lateral separation between the formation members is more than a wingspan of the leader aircraft. This formation geometry offers no drag benefit but has a strategic advantage. In the case of loose formation flight, the follower aircraft usually consumes more fuel than the leader aircraft because the follower aircraft should use more thrust to maintain the given formation geometry, especially during the join-up phase or the turning phase from the outside of the leader's flight path.

This note addresses the fuel saving problem of the follower aircraft in a loose formation, and a formation control scheme based on the energy maneuverability is proposed. In the energy maneuverability method that was proposed by Col. John Boyd [7], the kinetic and potential energy are exchanged to achieve the desired speed or height [8]. Thus, the thrust is only required to balance the energy dissipated by the aerodynamic drag along the path. In this study, it is assumed that the formation is composed of two aircraft. To design the proposed control law, the velocity command is designed using feedback linearization for the horizontal formation geometry [6] and then converted to the altitude command using the energy equation. A fuel consumption analysis is also performed. The fuel consumption of the follower aircraft is compared with that using the control scheme in Boskovic et al. [6].

Received 31 August 2007; revision received 15 January 2008; accepted for publication 6 February 2008.

*Graduate Student, School of Mechanical and Aerospace Engineering, Gwanak-ku; airchoi1@snu.ac.kr.

†Professor, School of Mechanical and Aerospace Engineering, the Institute of Advanced Aerospace Technology, Gwanak-ku; ydkim@snu.ac.kr. Senior Member AIAA.

II. Problem Formulation

A. System Dynamics

In this study, a three-dimensional point-mass model is considered for aircraft dynamics [9,10].

$$\dot{X}_i = V_i \cos\gamma_i \cos\chi_i \tag{1}$$

$$\dot{Y}_i = V_i \cos\gamma_i \sin\chi_i \tag{2}$$

$$\dot{H}_i = V_i \sin\gamma_i \tag{3}$$

$$\dot{\gamma}_i = \frac{-g\cos\gamma_i}{V_i} + \frac{a_{pi}}{V_i} \tag{4}$$

$$\dot{\chi}_i = \frac{a_{yi}}{V_i \cos\gamma_i} \tag{5}$$

where X_i and Y_i are the x and y direction position variables, H_i denotes the height, V_i is the velocity, and γ_i and χ_i are the flight-path angle and heading angle, respectively. Note that $i = 1$ represents the leader and $i = 2$ represents the follower aircraft. The aforementioned equation can be obtained with the assumptions of a constant weight, a point-mass aircraft with the thrust aligned along the velocity vector, a flat nonrotating Earth, and a constant gravitational attraction. The specific excess power represents the ability of the aircraft to change the energy state. The specific excess power may be used to change the altitude or accelerate the aircraft and is represented as [8]

$$P_{s_i} = \frac{V_i(T_i - D_i)}{W_i} \tag{6}$$

where T_i is the thrust, D_i is the aerodynamic drag, and W_i is the weight of the aircraft. The aircraft specific energy E_i represents the combined kinetic and potential energy of the vehicle per unit weight. The relationship between E_i and V_i can be derived from the energy state equation as

$$E_i = \frac{1}{W_i}\left(m_i g H_i + \frac{1}{2} m_i V_i^2\right) = H_i + \frac{V_i^2}{2g} \tag{7}$$

From Eq. (7), V_i can be written as

$$V_i = \sqrt{2g(E_i - H_i)} \tag{8}$$

Also, note that the aircraft specific excess power is equal to the rate of the aircraft specific energy and, therefore, the following relation is satisfied:

$$\frac{dE_i}{dt} = P_{s_i} = \frac{V_i(T_i - D_i)}{W_i} \tag{9}$$

The aerodynamic drag and propulsive force are modeled as

$$T_i = \eta_i T_{\max}(H) \tag{10}$$

$$D_i = D_{0i} + n^2 D_{ii} \tag{11}$$

In Eq. (11), the parasite drag D_{0i} and induced drag D_{ii} can be represented as

$$D_{0i} = qSC_{D_{0i}}, \qquad D_{ii} = k(W/qS)^2 \tag{12}$$

where q is the dynamic pressure, S is the wing area, $C_{D_{0i}}$ is the zero-lift drag coefficient, and k is the drag polar constant. The normalized throttle value η_i is modeled as the first-order delay as [11]

$$\dot{\eta}_i = -\frac{1}{\tau_\eta}\eta_i + \frac{1}{\tau_\eta}\eta_{ci}, \qquad \tau_{\eta_{\min}}(\eta_i) \le \tau_\eta \le \tau_{\eta_{\max}}(\eta_i) \tag{13}$$

where τ_η is the engine time constant, and $\eta_{ci}(0 \le \eta_{ci} \le 1)$ is the normalized throttle command value.

Consequently, Eqs. (1–5) and (9) are considered for the system dynamics, and the control variables in this study are the throttle command η_{ci}, the pitch acceleration a_{pi}, and the yaw acceleration a_{yi}.

B. Formation Geometry

The flight path of the formation flight usually lies on a horizontal plane and, therefore, it can be assumed that $\gamma_i \approx 0$. The formation flight control problem is decomposed into two decoupled problems: the horizontal tracking problem and vertical tracking problem. The horizontal relative position error in an inertial coordinate frame can be expressed as [6]

$$\begin{bmatrix} e_x \\ e_y \end{bmatrix} = \begin{bmatrix} X_1 - X_2 \\ Y_1 - Y_2 \end{bmatrix} - \begin{bmatrix} \cos(\chi_1) & -\sin(\chi_1) \\ \sin(\chi_1) & \cos(\chi_1) \end{bmatrix} \begin{bmatrix} x_d \\ y_d \end{bmatrix} \tag{14}$$

where χ_1 represents the heading angle of the leader aircraft, and subscript d denotes the desired relative distance.

The vertical distance error e_h is defined as

$$e_h = H_1 - H_2 - h_d, \qquad e_E = E_{d2} - E_2 \tag{15}$$

where h_d is the desired relative height difference, and E_d is the desired specific energy. The desired specific energy of the follower aircraft can be computed by using the speed and height information of the leader aircraft as

$$E_{d2} = H_1 + \frac{V_1^2}{2g} + h_d \tag{16}$$

C. Energy Maneuverability Based Formation Flight

Energy maneuverability involves the specification of the aircraft's climb and/or acceleration capability for various combinations of speed, altitude, and turning load factor. In other words, the potential energy can be exchanged with the kinetic energy to achieve the desired speed or height [8].

Differentiating Eq. (7) and using Eq. (3) gives the following relationship between $\dot{E}_i$ and $\dot{V}_i$:

$$\dot{E}_i = V_i(\sin\gamma_i + \dot{V}_i/g) \triangleq P_{si} \tag{17}$$

Assuming that the same energy level is maintained during flight, the following equation can be obtained for the constant energy level case, that is, $P_{si} = 0$:

$$\dot{V}_i = -g\sin\gamma_i \tag{18}$$

Note from Eq. (18) that the velocity can be changed by using the flight-path angle. This means that the aircraft must be in a level flight with constant speed, or in a climb while decelerating, or in a descent while accelerating to maintain a specified energy level. In other words, the velocity regulating the forward distance error can be obtained by exchanging the potential energy with the kinetic energy of the aircraft. During the energy transformation, however, some energy may be dissipated by the aerodynamic drag. To compensate for this energy loss, the throttle is used to maintain the energy level in this study. For example, if the follower aircraft is required to have V_{c2} to reduce the forward distance error e_x, then the follower aircraft has to approach the desired altitude H_{d2} by using the flight-path angle while regulating the specific energy error e_E. The desired altitude is obtained from the desired energy state E_{d2} and V_{c2} as

$$H_{d2} = E_{d2} - \frac{V_{c2}^2}{2g} \tag{19}$$

Figure 1 shows the schematic diagram of the proposed control concept.

III. Formation Control of Follower Aircraft

The control system of the follower aircraft consists of the command generator and autopilot, as shown in Fig. 2. It is assumed that the leader aircraft can generate the proper command signals to track the desired reference trajectory and, therefore, a second-order filter is used to produce the command signals V_{c1}, χ_{c1}, and H_{c1}.

A. Design of Follower Command

The "horizontal geometry" block computes the velocity command V_{c2} and heading angle command χ_{c2}. The computed commands are sent to the "state conversion" and "autopilot" blocks, respectively. To design the velocity and heading angle command generator, the autopilot dynamics are assumed to be the following first-order filters:

$$\dot{V}_2 = -\lambda_v(V_2 - V_{c2}) \tag{20}$$

$$\dot{\chi}_2 = -\lambda_\chi(\chi_2 - \chi_{c2}) \tag{21}$$

By differentiating Eqs. (1) and (2) and using the feedback linearization technique, the command generator can be designed as [6]

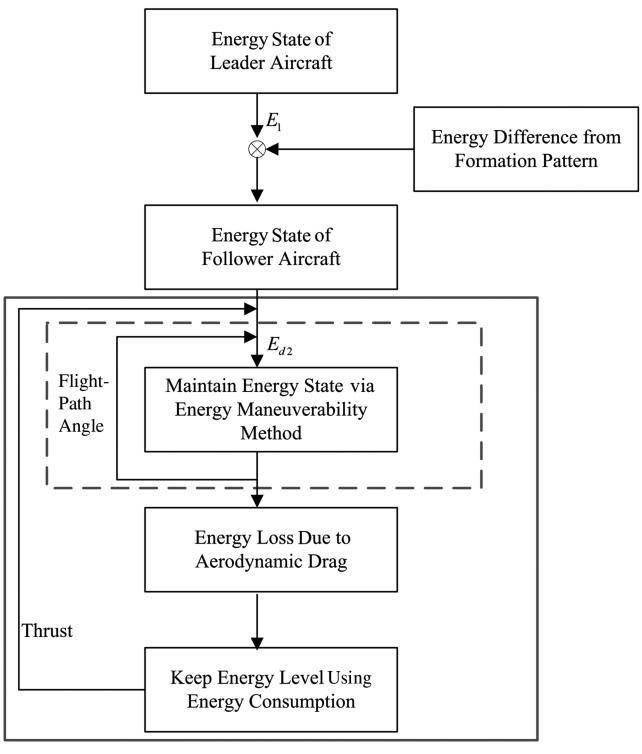

Fig. 1 Schematic diagram of the proposed control concept.

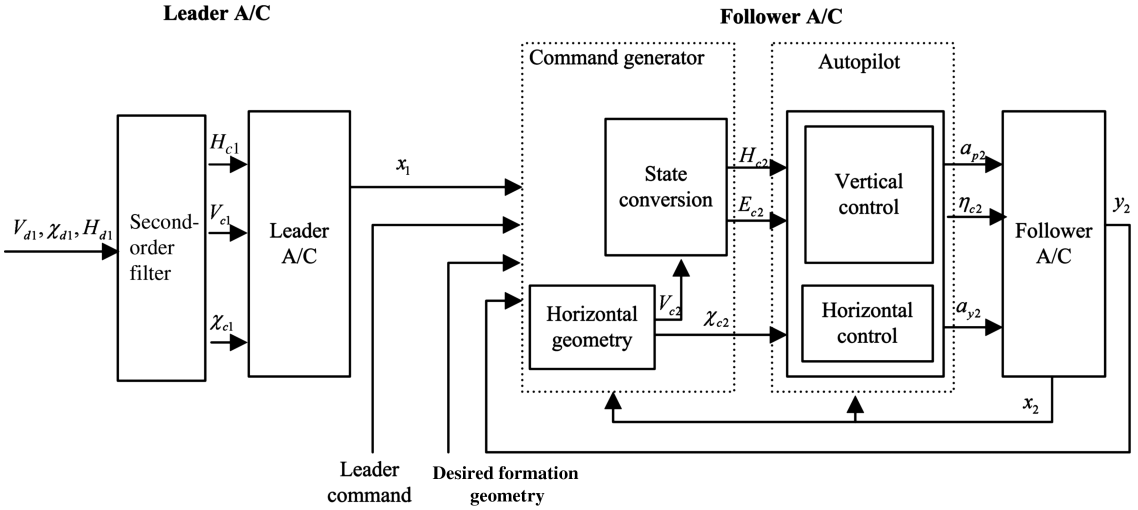

Fig. 2 Schematic diagram of the follower aircraft formation controller.

$$u = \begin{bmatrix} V_{c2} \\ \chi_{c2} \end{bmatrix} = G^{-1}[-f - k_1\dot{e} - k_2 e] \tag{22}$$

where $k_1 > 0$, $k_2 > 0$, and

$$f = \begin{bmatrix} \ddot{X}_1 + \lambda_v V_2 \cos\chi_2 - V_2 \sin\chi_2 \lambda_\chi \chi_2 \\ \ddot{Y}_1 + \lambda_v V_2 \sin\chi_2 + V_2 \cos\chi_2 \lambda_\chi \chi_2 \end{bmatrix} + \begin{bmatrix} \cos\chi_1 & -\sin\chi_1 \\ \sin\chi_1 & \cos\chi_1 \end{bmatrix} \begin{bmatrix} x_d \\ y_d \end{bmatrix} \dot{\chi}_1^2 \tag{23}$$

$$G = \begin{bmatrix} -\lambda_v \cos\chi_2 & \lambda_\chi V_2 \sin\chi_2 \\ -\lambda_v \sin\chi_2 & -\lambda_\chi V_2 \cos\chi_2 \end{bmatrix} \tag{24}$$

$$\ddot{X}_1 = \dot{V}_1 \cos\chi_1 - V_1 \sin\chi_1 \dot{\chi}_1 \qquad \ddot{Y}_i = \dot{V}_1 \sin\chi_1 + V_1 \cos\chi_1 \dot{\chi}_1 \tag{25}$$

The state conversion block computes the desired specific energy command E_{c2} and altitude command H_{c2} using Eqs. (16) and (19) and provides the computed values to the autopilot:

$$E_{c2} = H_1 + \frac{V_1^2}{2g} + h_d \tag{26}$$

$$H_{c2} = E_{c2} - \frac{V_{c2}^2}{2g} \tag{27}$$

B. Autopilot Design

The "vertical control" channel is designed by using the sliding control method. The output dynamics for the specific energy E_i and altitude H_i of each aircraft can be obtained by differentiating Eqs. (3) and (7) as

$$\ddot{E}_i = f_{Ei} + b_{Ei}\eta_{ci} \tag{28}$$

$$\ddot{H}_i = f_{Hi} + b_{Hi} a_{pi} \tag{29}$$

where

$$f_{Ei} = \frac{1}{W_i}\left(\left(\frac{\partial V_i}{\partial E_i}(T_i - D_i) - \frac{\partial D_i}{\partial E_i}V_i\right)\frac{V_i(T_i - D_i)}{W_i} + \left(\frac{\partial V_i}{\partial H_i}(T_i - D_i) - \frac{\partial D_i}{\partial H_i}V_i\right)V_i \sin\gamma_i + \frac{\partial T_i}{\partial \eta_i}V_i\right) \tag{30}$$

$$f_{Hi} = \frac{\partial V_i}{\partial E_i}\frac{V_i(T_i - D_i)}{W_i}\sin\gamma_i + \frac{\partial V_i}{\partial H_i}V_i \sin^2\gamma_i - g\cos^2\gamma_i \tag{31}$$

$$b_{Ei} = \frac{V_i}{W_i}\frac{\partial T_i}{\partial \eta_i}, \qquad b_{Hi} = \cos\gamma_i \tag{32}$$

Let us define the sliding surface as

$$s_{Ei} = \left(\frac{\mathrm{d}}{\mathrm{d}t} + \lambda_{Ei}\right)^2 \int_0^t e_{Ei}(\tau)\,\mathrm{d}\tau, \qquad e_{Ei}(\tau) = E_i - E_{ci} \tag{33}$$

$$s_{Hi} = \left(\frac{\mathrm{d}}{\mathrm{d}t} + \lambda_{Hi}\right)^2 \int_0^t e_{Hi}(\tau)\,\mathrm{d}\tau, \qquad e_{Hi}(\tau) = H_i - H_{ci} \tag{34}$$

where λ_{Ei} and λ_{Hi} are positive constants.

Differentiating s_{Ei} and s_{Hi}, we have

$$\begin{bmatrix} \dot{s}_{Ei} \\ \dot{s}_{Hi} \end{bmatrix} = \begin{bmatrix} v_{Ei} \\ v_{Hi} \end{bmatrix} + \begin{bmatrix} b_{Ei} & 0 \\ 0 & b_{Hi} \end{bmatrix} \begin{bmatrix} \eta_{ci} \\ a_{pi} \end{bmatrix} \tag{35}$$

where

$$v_{Ei} = -\ddot{E}_{ic} + f_{Ei} + 2\lambda_{Ei}\dot{e}_{Ei} + \lambda_{Ei}^2 e_{Ei} \tag{36}$$

$$v_{Hi} = -\ddot{H}_{ci} + f_{Hi} + 2\lambda_{Hi}\dot{e}_{Hi} + \lambda_{Hi}^2 e_{Hi} \tag{37}$$

Now, the control inputs can be determined such that the following sliding conditions are satisfied:

$$\frac{1}{2}\frac{\mathrm{d}}{\mathrm{d}t}s_{Ei}^2 \le -k_{Ei}|s_{Ei}| \tag{38}$$

$$\frac{1}{2}\frac{\mathrm{d}}{\mathrm{d}t}s_{Hi}^2 \le -k_{Hi}|s_{Hi}| \tag{39}$$

where k_{Ei} and k_{Hi} are positive constants. The controller that satisfies the aforementioned sliding conditions is obtained as

$$\begin{bmatrix} \eta_{ci} \\ a_{pi} \end{bmatrix} = B_i^{-1} \begin{bmatrix} -\nu_{Ei} - k_{Ei} sat(\frac{s_{Ei}}{\Phi_{Ei}}) \\ -\nu_{Hi} - k_{Hi} sat(\frac{s_{Hi}}{\Phi_{Hi}}) \end{bmatrix}, \qquad B_i = \begin{bmatrix} b_{Ei} & 0 \\ 0 & b_{Hi} \end{bmatrix} \tag{40}$$

where Φ_{Ei} and Φ_{Hi} are the widths of the boundary layer and $sat(s_{Ei}/\Phi_{Ei})$ is a continuous saturation function in which $sat(x) = x$ if $|x| \leq 1$ and $sat(x) = \text{sgn}(x)$ otherwise. Note that the inverse of B_i does exist for the entire flight envelop except for $V_i = 0$ or $\gamma_i = 90$ deg, which are unusual flight condition.

The horizontal control channel provides a_{y_i} to track the heading angle command χ_{ci} using proportion and integral control as

$$a_{y_2} = K_{ay_p} e_\chi + K_{ay_I} \int_0^t e_\chi \, \mathrm{d}t, \qquad e_\gamma = \chi_{c2} - \chi_2 \tag{41}$$

Remarks: In the proposed control scheme, the altitude should be changed to maintain formation geometry. The allowable altitude should be limited inside the flight envelop by considering the stall speed.

$$H_{2\min} \leq H_2 \leq H_2(V_{2s}) \tag{42}$$

where $H_2(V_{2s})$ can be calculated as

$$H_2(V_{2s}) = E_2 - \frac{V_{2s}^2}{2g} \tag{43}$$

IV. Fuel Consumption Analysis

To examine the performance of the proposed controller, a fuel consumption analysis is performed. The weight change rate can be represented as a function of the specific fuel consumption as [12]

$$\frac{\mathrm{d}W}{\mathrm{d}t} = -\frac{\mathrm{d}W_F}{\mathrm{d}t} = -\text{TSFC} \times T \tag{44}$$

where W_F is the weight of the fuel, and TSFC is the installed thrust specific fuel consumption, which is defined as

$$\text{TSFC} = C\sqrt{\theta} \tag{45}$$

where C is a specific fuel consumption and θ is a static temperature ratio.

The fuel consumption can be analyzed for the two different thrust loading behavior cases. In case A, the specific excess power (P_s) is more than zero ($P_s > 0$) and, in case B, $P_s = 0$. Case A corresponds to the case of constant speed clime, horizontal acceleration, etc., and case B corresponds to the case of constant speed cruise, constant energy maneuver, etc. Let us compare the fuel consumption between the horizontal acceleration case with $P_s > 0$ and the acceleration case with a constant energy maneuver with $P_s = 0$.

Case A: This horizontal acceleration case ($P_s > 0$) corresponds to the situation in which the thrust is used to accelerate. For this case, the weight fraction can be calculated by [12]

$$\left(\frac{W_f}{W_i}\right)_{P_s>0} \triangleq \left(\frac{W_f}{W_i}\right)_a = \exp\left\{-\frac{C_a\sqrt{\theta_a}}{V_a} \frac{\Delta(V_a^2/2g)}{1-(C_{D_a}/C_{L_a})(W_a/T_a)}\right\} \tag{46}$$

where W_i and W_f are the initial and final weight of aircraft.

Case B: This acceleration case with a constant energy maneuver ($P_s = 0$) corresponds to the situation in which the potential energy is exchanged with the kinetic energy for acceleration during descent. The weight fraction can be calculated by [12]

$$\left(\frac{W_f}{W_i}\right)_{P_s=0} \triangleq \left(\frac{W_f}{W_i}\right)_b = \exp\left\{-C_b\sqrt{\theta_b}\frac{C_{D_b}}{C_{L_b}}\Delta t_b\right\} \tag{47}$$

where the maneuver time interval Δt_b is obtained by recognizing that the maneuver distance is $h_{b_{\text{final}}} - h_{b_{\text{initial}}}$ and assuming that the vertical speed is some fraction of the average speed $(V_{b_{\text{final}}} + V_{b_{\text{initial}}})/2$.

Assume that the consumed fuel of case B is less than that of case A. Then, the following relation is obtained by using Eqs. (46) and (47):

$$\frac{C_a\sqrt{\theta_a}}{V_a} \frac{\Delta(V_a^2/2g)}{1-(C_{D_a}/C_{L_a})(W_a/T_a)} - C_b\sqrt{\theta_b}\frac{C_{D_b}}{C_{L_b}}\Delta t_b > 0 \tag{48}$$

Let us define K_a and K_b as

$$K_a \triangleq \frac{\sqrt{\theta_a}}{1-(C_{D_a}/C_{L_a})(W_a/T_a)}, \qquad K_b \triangleq \sqrt{\theta_b}\frac{C_{D_b}}{C_{L_b}} \tag{49}$$

In the acceleration case considered in this study, we have

$$0 < 1 - \frac{C_{D_a}}{C_{L_a}}\frac{W_a}{T_a} < 1 \tag{50}$$

Using Eq. (50) in Eq. (49), $K_a > 0$ and also $K_b > 0$. Using the average value for V_a and V_b and substituting Eq. (49) into Eq. (48) yields

$$\frac{C_a K_a}{V_{a_{\text{final}}} + V_{a_{\text{initial}}}} \frac{1}{g}(V_{a_{\text{final}}}^2 - V_{a_{\text{initial}}}^2) - C_b K_b \frac{2|h_{b_{\text{final}}} - h_{b_{\text{initial}}}|}{V_{b_{\text{final}}} + V_{b_{\text{initial}}}} > 0 \tag{51}$$

For comparison, let us consider that the initial and final speeds of cases A and B are the same:

$$V_{a_{\text{initial}}} = V_{b_{\text{initial}}} = V_{\text{initial}} \qquad V_{a_{\text{final}}} = V_{b_{\text{final}}} = V_{\text{final}} \tag{52}$$

For case B, the energy level is the same and, therefore, we have

$$|h_{b_{\text{final}}} - h_{b_{\text{initial}}}| = \frac{1}{2g}(V_{\text{final}}^2 - V_{\text{initial}}^2) \tag{53}$$

Using Eqs. (52) and (53) in Eq. (51), the following condition can be obtained:

$$\frac{C_a K_a}{C_b K_b} > 1 \tag{54}$$

Because the specific fuel consumption C_a and C_b for cases A and B are positive values depending mainly on the Mach number [8], it can be assumed that $C_a \approx C_b$. Note from K_a and $K_b > 0$ that Eq. (54) is true if the following condition is satisfied:

$$\frac{\min K_a}{\max K_b} > 1 \tag{55}$$

Using Eq. (50) in Eq. (55), the following condition can be obtained:

$$\frac{\min K_a}{\max K_b} \geq \frac{\sqrt{\theta_a}}{\max(K_b)} = \sqrt{\frac{\theta_a}{\theta_b}} \min\left(\frac{C_{L_b}}{C_{D_b}}\right) > 1 \tag{56}$$

Assuming that the static temperature ratios $\theta_a \approx \theta_b$, the following condition is derived:

$$\min\left(\frac{C_{L_b}}{C_{D_b}}\right) > 1 \tag{57}$$

Because this condition is satisfied for most flight conditions, the assumption that the consumed fuel of case B is less than that of case A is true. Note that case B corresponds to the maneuver using the energy maneuverability concept.

V. Numerical Simulation

Numerical simulations are performed to verify the performance of the proposed controller (control 1). The simulation results are compared with those of another reference controller that does not use the energy maneuverability theory (control 2). To compare the fuel consumption at the same error performance, control 2 is composed of the command generator [6] for generating the speed and heading command signals and the command generator for generating the following:

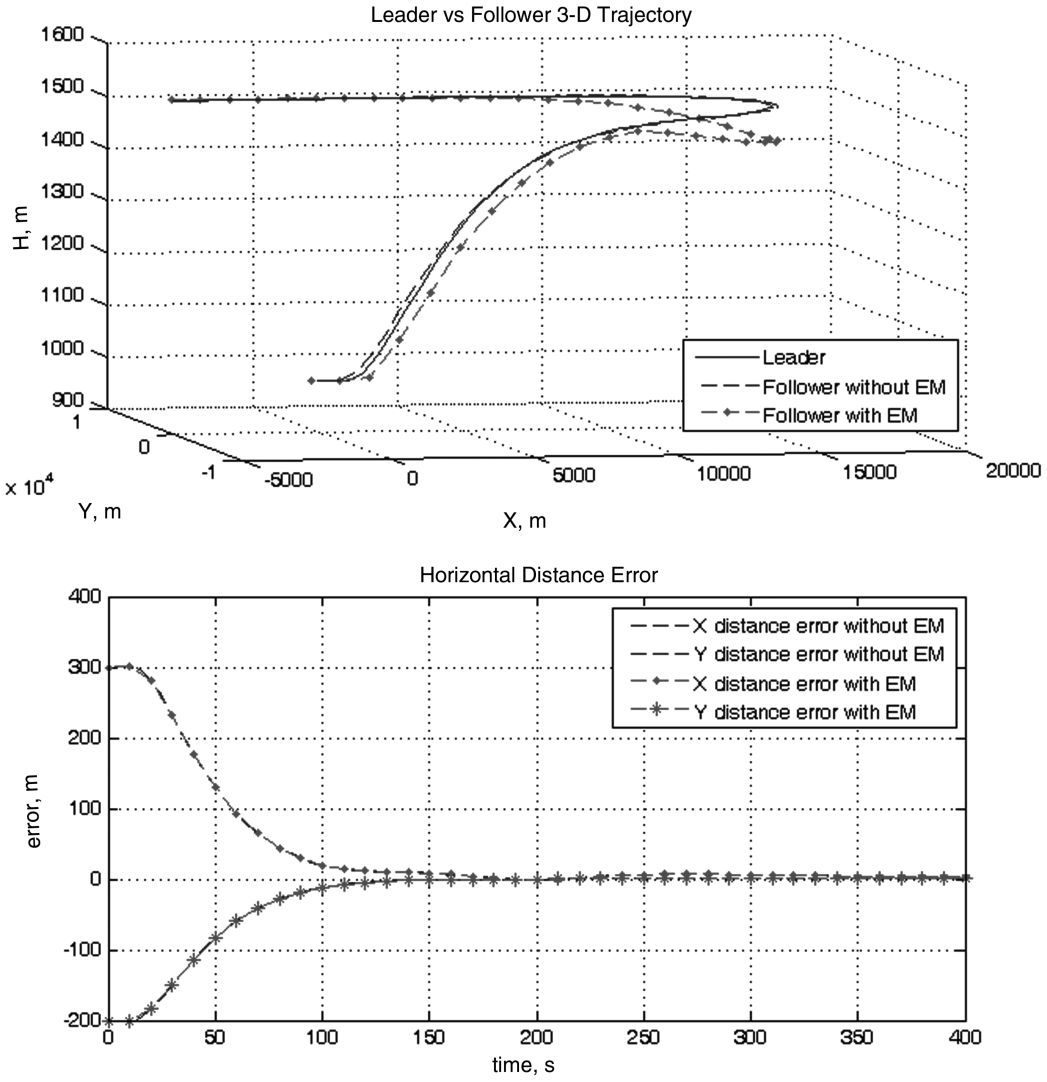

Fig. 3 Leader and follower trajectories and distance error.

$$E_{c2_{\text{woEM}}} = H_1 + \frac{V_{c2}^2}{2g} + h_d, \qquad H_{c2_{\text{woEM}}} = H_1 + h_d \tag{58}$$

Note that Eq. (58) does not reflect the kinetic and potential energy exchange.

The initial positions of the leader and the follower are chosen as $[0 \quad 0 \quad 1000]^T$ m and $[-300 \quad 0 \quad 1000]^T$ m, respectively. The initial speeds of the leader and the follower are 100 m/s, and the desired relative distance of the follower is set at $[0 \quad 200 \quad 0]^T$ m. The aircraft parameters and the TSFC model are adopted from Raymer [8] and Segal et al. [13], respectively. The engine model is adopted from Stevens and Lewis [11]. The control parameters chosen for the simulation are $\lambda_v = 5$ and $\lambda_\chi = 10$ (command generator); $\lambda_E = 5$, $k_E = 0.1$, $\Phi_E = 1$, $\lambda_H = 5$, $k_H = 0.1$ and $\Phi_H = 0.1$ (vertical control); and $k_{\chi_p} = 100$ and $k_{\chi_i} = 1$ (horizontal control).

As a result of the simulation, the total energy usage

$$E_{\text{total}} = \int_0^t E \, \mathrm{d}t$$

of each control is 779,080 ft (control 1) and 788,752 ft (control 2), respectively. The fuel consumption of each control is 297.2 kg (control 1) and 300.4 kg (control 2), respectively. By comparing these results, the total energy usage and fuel consumption of control 1 is less than that of control 2. And the difference in the fuel consumption at the final time is 3.2 kg for the 400 s flight. Figure 3 shows the trajectory and horizontal distance error history of the two controllers. As shown in Fig. 3, control 1 performs the energy maneuver during the turn phase, and the horizontal errors have almost same values for the two controllers.

VI. Conclusions

In this note, a formation flight controller based on the energy maneuverability concept is proposed. A fuel consumption analysis showed that the controller using the energy maneuverability method spends less fuel than the controller using the thrust as a main actuator. A numerical simulation was performed to verify the effectiveness of the proposed method. The result of the numerical simulation showed that the fuel consumption using the energy maneuverability method was less than that without using the energy maneuverability method in the loose formation geometry. Note that the proposed controller forces the follower aircraft to change its altitude to maintain the formation geometry. Therefore, the proposed controller may be more useful for a formation geometry that requires a large relative distance between the leader and follower aircraft than for a tight formation geometry.

Acknowledgment

This work was supported by the Korea Science and Engineering Foundation (KOSEF) grant funded by the Korean government (MOST) (no. ROA-2007-000-10017-0).

References

[1] Hummel, D., "The Use of Aircraft Wakes to Achieve Power Reductions in Formation Flight," *The Characterisation & Modification of Wakes from Lifting Vehicles in Fluids*, CP-584, AGARD, Neuilly-sur-Seine, France, 1996, pp. 36.1–36.13.

[2] Wagner, G., Jacques, D., Blake, W., and Pachter, M., "Flight Test Results of Close Formation Flight for Fuel Savings," AIAA Paper 2002-4490, Aug. 2002.

[3] Wagner, G., Jacques, D., Blake, W., and Pachter, M., "An Analytical Study of Drag Reduction in Tight Formation Flight," AIAA Paper 2001-4075, Aug. 2001.

[4] Pachter, M., D'Azzo, J. J., and Proud, A. W., "Tight Formation Flight Control," *Journal of Guidance, Control, and Dynamics*, Vol. 24, No. 2, 2001, pp. 246–254.

[5] Chichka, D. F., Speyer, J. L., Fanti, D., and Park, C. G., "Peak-Seeking Control for Drag Reduction in Formation Flight," *Journal of Guidance, Control, and Dynamics*, Vol. 29, No. 5, 2006, pp. 1221–1230. doi:10.2514/1.15424

[6] Boskovic, J. D., Li, S.-M., and Mehra, R. K., "Semi-Globally Stable Formation Flight Control Design in Three Dimensions," *Proceedings of the 40th IEEE Conference on Decision and Control*, Institute of Electrical and Electronics Engineers, Piscataway, NJ, Dec. 2001, pp. 1059–1064.

[7] Coram, R., *Boyd: The Fighter Pilot Who Changed the Art of War*, Back Bay Books, New York, 2002, p. 135.

[8] Raymer, D. P., *Aircraft Design: A Conceptual Approach*, AIAA, Washington, D.C., 1989, Chaps. 3, 17, Appendix A.4-2.

[9] Visser, H. G., Kelley, H. J., and Cliff, E. M., "Energy Management of Three-Dimensional Minimum-Time Intercept," *Journal of Guidance, Control, and Dynamics*, Vol. 10, No. 6, 1987, pp. 574–580.

[10] Rajan, N., and Ardema, M. D., "Interception in Three Dimensions: An Energy Formulation," *Journal of Guidance, Control, and Dynamics*, Vol. 8, No. 1, 1985, pp. 23–30.

[11] Stevens, B. L., and Lewis, F. L., *Aircraft Control and Simulation*, 2nd ed., Wiley, Hoboken, NJ, 2003, pp. 634–635.

[12] Mattingly, J. D., Geiser, W. H., and Daley, D. H., *Aircraft Engine Design*, AIAA, Washington, D.C., 1987, pp. 53–69.

[13] Segal, S., Ben-Asher, J. Z., and Weiss, H., "Derivation of Formation–Flight Guidance Laws for Unmanned Air Vehicles," *Journal of Guidance, Control, and Dynamics*, Vol. 28, No. 4, 2005, pp. 733–742. doi:10.2514/1.7420